Accepted Manuscript

Title: Folate-targeted amphiphilic cyclodextrin nanoparticles incorporating a fusogenic peptide deliver therapeutic siRNA and inhibit the invasive capacity of 3D prostate cancer tumours

Authors: James C. Evans, Meenakshi Malhotra, Katrina Sweeney, Raphael Darcy, Colleen C. Nelson, Brett G. Hollier, Caitriona M. O'Driscoll

PII: S0378-5173(17)30868-2
DOI: http://dx.doi.org/10.1016/j.ijpharm.2017.09.013
Reference: IJP 16994

To appear in: *International Journal of Pharmaceutics*

Received date: 5-4-2017
Revised date: 5-9-2017
Accepted date: 7-9-2017

Please cite this article as: Evans, James C., Malhotra, Meenakshi, Sweeney, Katrina, Darcy, Raphael, Nelson, Colleen C., Hollier, Brett G., O'Driscoll, Caitriona M., Folate-targeted amphiphilic cyclodextrin nanoparticles incorporating a fusogenic peptide deliver therapeutic siRNA and inhibit the invasive capacity of 3D prostate cancer tumours.International Journal of Pharmaceutics http://dx.doi.org/10.1016/j.ijpharm.2017.09.013

Folate-targeted amphiphilic cyclodextrin nanoparticles incorporating a fusogenic peptide deliver therapeutic siRNA and inhibit the invasive capacity of 3D prostate cancer tumours

Authors
James C. Evans[1]
Meenakshi Malhotra[1]
Katrina Sweeney[2]
Raphael Darcy[1]
Colleen C. Nelson[2]
Brett G. Hollier[2]
Caitriona M. O'Driscoll[1]
[1]Pharmacodelivery Group, School of Pharmacy, University College Cork, Cork, Ireland.
[2]Australian Prostate Cancer Research Centre - Queensland, Institute of Health and Biomedical Innovation, Queensland University of Technology, Princess Alexandra Hospital, Translational Research Institute, Brisbane, Australia.
All correspondence relating to this paper should be addressed to:
Professor Caitriona O'Driscoll,
School of Pharmacy,
University College Cork,
Ireland.
Tel: +353-21-4901396
Fax: +353-21-4901656
E-mail:caitriona.odriscoll@ucc.ie

Graphical Abstract

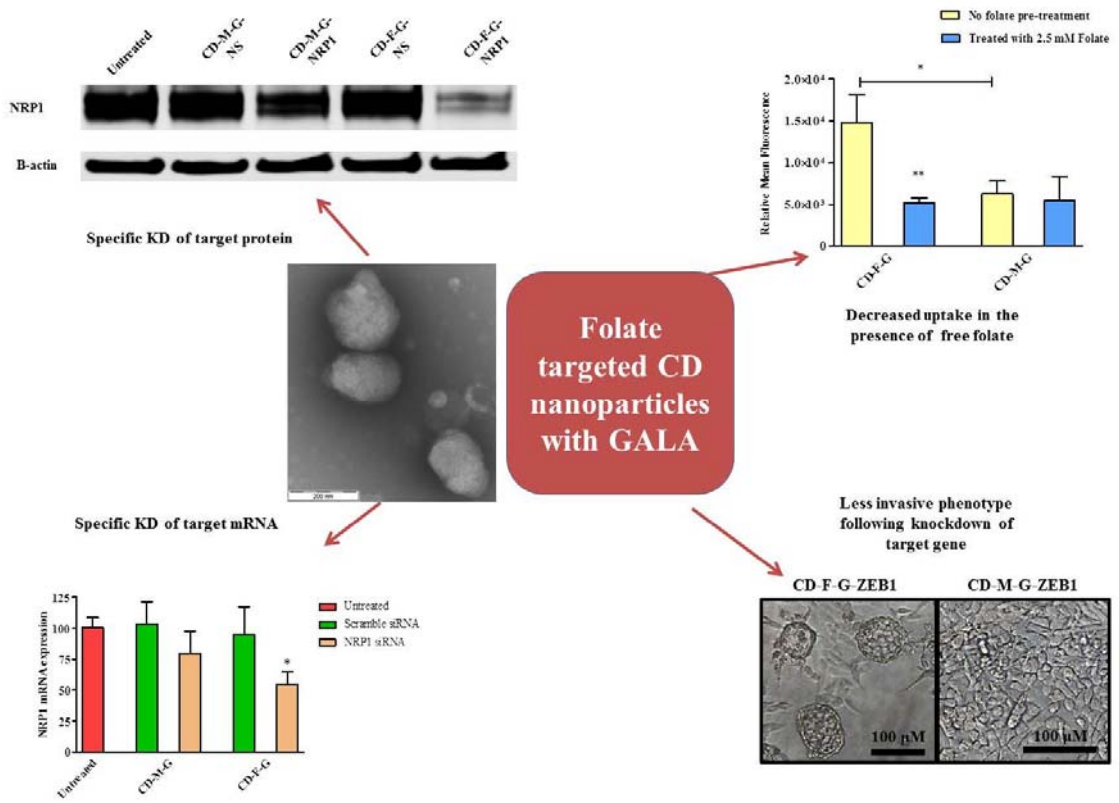

Abstract

The main barrier to the development of an effective RNA interference (RNAi) therapy is the lack of a suitable delivery vector. Modified cyclodextrins have emerged in recent years for the delivery of siRNA. In the present study, a folate-targeted amphiphilic cyclodextrin was formulated using DSPE-PEG$_{5000}$-folate to target prostate cancer cells. The fusogenic peptide GALA was included in the formulation to aid in the endosomal release of siRNA. Targeted nanoparticles were less than 200 nm in size with a neutral surface charge. The complexes were able to bind siRNA and protect it from serum nucleases. Incubation with excess free folate resulted in a significant decrease in the uptake of targeted nanoparticles in LNCaP and PC3 cells, both of which have been reported to have differing pathways of folate uptake. There was a significant reduction in the therapeutic targets, ZEB1 and NRP1 at mRNA and protein level following treatment with targeted complexes. In preliminary functional assays using 3D spheroids, treatment of PC3 tumours with targeted complexes with ZEB1 and NRP1 siRNA

resulted in more compact colonies relative to the untargeted controls and inhibited infiltration into the Matrigel™ layer.

Keywords: RNAi; Cyclodextrin; GALA; siRNA delivery; prostate cancer; metastasis; folate

1. Introduction

Prostate cancer is the most prevalent cancer diagnosed in men of the western world (in the US, an estimated 220,000 new cases were diagnosed in 2015), with current treatments for the metastatic disease offering only a modest increase in survival (Siegel et al., 2015). Since its discovery, RNA interference (RNAi) has been considered as an effective potential therapeutic for a wide range of diseases, including, but not limited to, cancer. The uptake and targeted delivery of the large, anionic siRNA is the main barrier to the development of effective RNAi therapeutics (Wittrup and Lieberman, 2015). In 2003, the first proof of principle of RNAi therapeutics emerged where siRNAs were shown to successfully treat disease in an *in vivo* model where the delivery of naked *Fas* siRNA protected mice from autoimmune hepatitis (Song et al., 2003).

Cyclodextrins (CD) are a family of cyclic oligosaccharides with a history of use as pharmaceutical excipients (Jambhekar and Breen, 2016a, b). As well as acting as solubilizers and stabilizers in drug formulations, modified cyclodextrins can act as carriers of large complex molecules, such as nucleic acids and proteins (A do Carmo et al., 2014; Aranda et al., 2013; Meredith et al., 2015). In fact, the first example of targeted delivery of siRNA in humans was using a cyclodextrin containing polymer (CDP) as a delivery vector (Davis, 2009). In this study, CDP vectors containing siRNA targeting M2 subunit of ribonucleotide reductase (MMR2) were targeted to tumours using the transferrin moiety, termed CALAA-01 (Davis, 2009). Since the emergence of CALAA-01, cyclodextrins have emerged as an effective vector

for delivering siRNA in a variety of diseases including prostate cancer and neurological disorders (Evans et al., 2015; Fitzgerald et al., 2016; Guo et al., 2012; O'Mahony et al., 2012b).

In a recent study, an amphiphilic CD formulated with DSPE-PEG_{5000}-folate to target PSMA in prostate cancer cells resulted in a significant reduction in RelA mRNA (knockdown of RelA has previously been shown to reduce the metastatic potential of PC3 cells (Evans et al., 2015)) in PSMA-positive cells compared with non-silencing and untargeted controls (Evans et al., 2016b). The incorporation of DSPE-PEG_{5000}-folate into pre-formed CD.siRNA nanoparticles resulted in an improved pharmacokinetic profile of siRNA, with significant increases in half-life ($t_{1/2}$), area under the curve (AUC) and clearance compared with naked siRNA (Evans et al., 2016b).

Following successful uptake and internalisation of siRNA containing nanoparticles into cells, inefficient endosomal escape can hinder any therapeutic benefit. GALA is a 30 amino acid endosomal escape peptide (*WEAALAEALAEALAEHLAEALAEALEALAA*) that is derived from viral proteins that enhances endosomal release following its uptake (Li et al., 2004; Parente et al., 1990). The composition of the GALA peptide is repetitive units of Glu-Ala-Leu-Ala. Subbarao et al demonstrated that at a low pH (such as the environment of the endosome), the GALA peptide transitions from a random coil structure to a α-helical structure, which exposes a hydrophobic face in the peptide. This transition was confirmed by circular dichroism. Association of the GALA peptide with a bilayer at low pH was confirmed by measuring the shift in fluorescence of a tryptophan residue at the terminal end of the peptide following incubation at pH 5 (Subbarao et al., 1987). The addition of GALA to cationic nanoparticles has been shown to improve their endosomal escape (Simoes et al., 1998; Simoes et al., 1999a; Simoes et al., 1999b).

Epithelial to mesenchymal transition (EMT) is a fundamental developmental process that occurs during embryogenesis (Hay, 1995). This process has been well documented as being reactivated in many disease states including cancer, with EMT shown to regulate cancer metastasis and chemoresistance (Fischer et al., 2015; Yao et al., 2011; Zheng et al., 2015). The transcription factor zinc finger E-box-binding homeobox 1 (ZEB1) has been shown to induce EMT by direct downregulation of E-cadherin (Zhang et al., 2015). Neuropilin-1 (NRP-1) is a transmembrane glycoprotein that interacts with members of the VEGF family to promote angiogenesis (Graziani and Lacal, 2015; Pellet-Many et al., 2008). NRP1 expression has been shown to be upregulated in metastatic prostate cancer compared with localized prostate cancer (Latil et al., 2000; Yacoub et al., 2009). Consequently, the silencing of these genes using siRNA may have significant therapeutic potential.

Previously, a folate targeted CD nanoparticle (NP) was formulated for siRNA delivery to prostate cancer (Evans et al., 2016b). However, the CD used in this case was an "inverted" SC_8CDcysteamine which contained cationic amine groups on its primary face and C_8 lipophilic chains on the secondary face (O'Mahony et al., 2012a). For the current study, an alternative amphiphilic SC_{12}CDclickpropylamine CD (cationic groups on the secondary face and C_{12} on the primary face) was used, which has shown great therapeutic potential for siRNA delivery in a wide variety of disease states including Huntington's disease and inflammatory bowel disease (Godinho et al., 2013; McCarthy et al., 2013). The primary aim of this study was to formulate a folate-targeted CD with the fusogenic peptide GALA in order to facilitate enhanced endosomal escape. DSPE-PEG_{5000}-folate and the GALA peptide were post-inserted into preformed CD.siRNA complexes. The physicochemical properties of the nanoparticles were assessed as well as their ability to achieve targeted delivery in prostate cancer cells *in vitro.* The complexes were used to deliver ZEB1 and NRP1 siRNA into prostate cancer cells and knockdown was assessed using RT-PCR and western blot analysis. Preliminary functional

studies were carried out by assessing the invasive capacity of 3D PC3 spheroids following knockdown of ZEB1 and NRP1.

2. Materials and methods

2.1.Materials

GALA peptide was purchased from AnaSpec (Fremont, CA). ZEB1, NRP1 and negative control siRNA were purchased from ThermoFisher Scientific (Waltham, MA). FLuciferase siRNA was custom synthesized by IDT (Coralville, IA) with the following sequence: (sense 5'-GGGGGACGAGGACGAGCACUTC-3'). Negative control 6-carboxyfluorescein (6-FAM)-labelled siRNA was purchased from Sigma Aldrich (St. Louis, MO) Amphiphilic SC_{12}CDclickpropylamine cyclodextrin was synthesized as previously described (O'Mahony et al., 2012b). DSPE-PEG_{5000}-folate (DPF) and DSPE-PEG_{5000}-methyl (DPM) were purchased from Nanocs (New York, NY).

2.2.Preparation of CD.siRNA nanoparticles

CD and siRNA nanoparticles at a mass ratio (MR) of CD:siRNA of 20:1 were prepared as previously described (Evans et al., 2015). Briefly, siRNA and CD were mixed at MR20 at room temperature, vortexed lightly for 10-15 sec, and left to form electrostatic interactions for 25-30 minutes. DSPE-PEG_{5000} reagents (i.e. DSPE-PEG_{5000}-methyl and DSPE-PEG_{5000}-folate) were dissolved in water to 1 mg/ml. GALA peptide was dissolved in 1% NH_4OH to 0.25 mg/ml. DSPE-PEG_{5000} reagents and GALA were mixed together and added to preformed CD.siRNA nanoparticles by the post-insertion method previously reported [REF]. Resulting mixtures were heated to 60°C for 15 mins at 500 rpm in a thermomixer. The exact composition of each formulation is described in in **Table 1.**

2.3.Particle size and zeta potential (ζ)

Particle size and zeta potential (ζ) of cyclodextrin nanoparticles were measured using a Malvern Zeta Sizer (Malvern, Worcestershire, UK) as previously described (Evans et al., 2016b).

2.4.Transmission electron microscopy (TEM)

Complexes were made as described above and added to 400 mesh carbon-film copper grids (Agar Scientific, Essex, UK). Grids were stained with 2 % (w/v) uranyl acetate, left to dry and images taken using a JEOL 2000 FXII transmission electron microscope (Jel Ltd., Tokyo, Japan).

2.5.Binding Assay

Complexes were formed as above and run on a 1.5 % agarose gel at 120 V in Tris/Borate/EDTA (TBE) for 30 minutes supplemented with 0.06 % v/v SafeView nucleic acid stain (NBS Biologicals). UV light was used to visualize unbound siRNA.

2.6.Assessment of nanoparticles in physiological conditions

Serum stability studies were carried out in 10 % FBS at 0 min, 3 min, 15 min, 1 h, 4h and 8 h as previously described (Evans et al., 2016b). For the aggregation study, nanoparticles were incubated in 90 % optiMEM® for up to 4 h. The count rate of the solutions at each of the time points was determined using a Malvern Zeta Sizer (Malvern, Worcestershire, UK).

2.7.Cell culture

PC3 and LNCaP cells were provided by the Australian Prostate Cancer Research Centre Queensland (APCRC-Q), purchased previously from the American Type Culture Collection (ATCC, Manassas, VA, USA) and maintained in phenol-red free RPMI 1640 supplemented with 5 % FBS. Both cell lines were grown in the Forma Series II Water Jacketed CO_2 incubator

(Thermo Electron Corporation, Waltham, Massachusetts) at 37°C with 5 % CO_2 and 95 % relative humidity.

2.8.MTT assay

1 x 10^4 PC3 and LNCaP cells were seeded into 96 well plates 24 h prior to transfection. Cells were transfected with cationic CD (CCD), CD-DSPE-PEG_{5000}-Folate-GALA (CD-F-G) and CD-DSPE-PEG_{5000}-Methyl-GALA (CD-M-G) complexes for 24 h. Following this time, complexes were removed and cells were incubated with MTT solution (0.5mg/ml) for 4 hours. Resulting formazoan crystals were dissolved in DMSO and absorbance was read using a multiplate reader at 590 nm (Perkin Elmer – Wallac Victor2™ 1420 multiplate counter).

2.9.Competition assay

1 x 10^4 PC3 and LNCaP cells were seeded into a black 96-well plate. Cyclodextrin complexes with 50 nM 6-FAM-labelled siRNA were formulated as described above. Cells were pre-incubated with 2.5 mM folic acid for 1 hour prior to the addition of the complexes. Complexes were left on cells for 4 h. Cells were washed twice with PBS to remove any unbound complexes. Cell uptake was determined by measuring fluorescence intensity using a Perkin Elmer Victor2 1420 fluorescent plate reader (excitation 485 nm, emission 535 nm).

2.10. Luciferase assay

1 x 10^4 $PC3^{Luc}$ cells (engineered to express luciferase) were seeded in opaque white 96-well plates (Corning Inc., NY) 24 h prior to transfection. Cells were transfected with either Lipofectamine2000 (LIPO) or CD complexed with 100 nM negative control siRNA or luciferase siRNA for 48 h. D-luciferin (PerkinElmer, Waltham, MA) was added to cells and luminescence was determined using a multiplate reader at 560 nm (Perkin Elmer – Wallac Victor2™ 1420 multiplate counter).

2.11. 3D spheroid invasion assay

1 x 10^3 PC3 cells were seeded onto the surface of undiluted Matrigel™ in phenol-red free RPMI1640 containing 2.5 % (v/v) Matrigel™. Following the formation of spheroids (typically 3-4 days), cells were treated with CD-F-G and CD-M-G nanoparticles at t= 0 h and t= 48 h at a final siRNA concentration on 100 nM.

2.12. Quantitative real-time (RT) PCR

24 h prior to transfection, 5 x 10^4 PC3 and LNCaP cells were seeded in 24 well plates. Cells were transfected with CD.siRNA complexes for 24 h and RNA was extracted using Direct-zol™ RNA kit (Zymo Research, Australia). 300 ng of RNA was used to synthesize cDNA using SensiFAST™ cDNA synthesis kits (Bioline, UK). RT-PCR was carried out using SYBR Green (Applied Biosystems, Foster City, CA) and ViiA 7 Real Time PCR system (Applied Biosystems, Foster City, CA). Primers targeting ZEB1 (Primer sequence; forward: CAACTACGGTCAGCCCT, reverse: GCGGTGTAGAATCAGAGTC), NRP1 (Primer sequence; forward: AGGACAGAGACTGCAAGTATGAC, reverse: AACATTCAGGACCTCTCTTGA) and the house keeping gene RPL32 (Primer sequence; forward: GCACCAGTCAGACCGATATG, reverse: ACTGGGCAGCATGTGCTTTG) were used and gene expression determined by the comparative Ct method.

2.13. Western blot analysis

24 h prior to transfection, 2.5 x 10^5 PC3 cells were seeded in 6 well plates. Cells were transfected with CD.siRNA complexes for 48 h and lysed using RIPA (Radio-Immunoprecipitation Assay) buffer with protease inhibitor cocktail (P8340) (Sigma). Protein concentrations were quantified using the BCA assay. 30µg of the total protein was loaded onto a 4-12% gradient BOLT® gel (Thermo Fisher Scientific, Waltham, MA) and run at 150 V after which proteins were transferred onto a nitrocellulose membrane. Western blotting was carried

out using antibodies to NRP1 (sc-7239, Santa Cruz Biotechnology), ZEB1 (3396, Cell Signalling Technologies) and β-actin (sc-7239, Santa Cruz Biotechnology). Signals were detected using Infrared secondary antibodies and the Licor Odyssey® Infrared imaging system (Lincoln, NE).

2.14. Statistical analysis

Data were expressed as mean ± standard deviation (SD) of at least triplicate samples. One-way Analysis of Variance (ANOVA) was performed to test the significance of differences in three or more groups followed by Tukey's Post-Hoc test and a two-tailed unpaired student *t*-test was used to compare significance of differences in two groups. In all cases, $P < 0.05$ was considered to be statistically significant. All graphs and statistical calculations were prepared using GraphPad Prism 5 (San Diego, CA).

3. Results and discussion

3.1 CD-F-G nanoparticles display favourable physicochemical properties and are capable of binding and protecting siRNA from serum nucleases.

Four different cyclodextrin formulations were investigated in this study:

Formulation one was a cationic amphiphilic CD complexed with siRNA (hereafter referred to as CCD).

Formulation two was a targeted NP containing CCD co-formulated with a blend of DSPE-PEG_{5000}-folate (DPF) and GALA peptide (hereafter referred to as CD-F-G).

Formulation three was a targeted NP containing CCD co-formulated with DSPE-PEG_{5000}-folate (DPF) (hereafter referred to as CD-F)

Formulation four was the untargeted NP control containing CCD with DSPE-PEG_{5000} (DPM) and GALA (referred to as CD-M-G).

Screening studies were performed in order to determine the optimal molar ratio of CD:DSPE-PEG:GALA (**Supplementary Table 1**). The exact composition, particle size, zeta potential and PDI of each formulation is given in **Table 1**.

The amphiphilic CD used in this study has previously been shown to be capable of fully complexing siRNA from mass ratio 5 (MR 5) and above (Godinho et al., 2013). It was therefore necessary to test whether the addition of DSPE-PEG_{5000} alone or in combination with the amphiphilic peptide GALA to the formulation would displace the bound siRNA. As can be seen in **Figure 1a**, naked siRNA (i) has migrated through the gel, but for the three formulations tested (i.e. CCD, CD-F-G and CD-M-G), there was no siRNA band detected, highlighting that in these cases, siRNA is bound by the CD complexes. This result confirms that all three complexes were capable of binding siRNA efficiently.

The potential for the nanoparticles to aggregate in a salt-containing medium was also investigated. The addition of PEG is used to confer "steric" stability to nanoparticles (Gref et al., 2000; Monfardini and Veronese, 1998). Recent studies have shown that incorporation of PEG of various lengths (500, 1000, 2000 and 5000) increases the stability of cyclodextrin containing nanoparticles and increased the $t_{1/2}$ of siRNA *in vivo* (Evans et al., 2016b; Godinho et al., 2014b). The diameter of CCD and CD-F-G (measured by dynamic light scattering (DLS)) was determined over a 24 h period following the addition of optiMEM® (**Figure 1 b**). In the case of unPEGylated CCD, there was a dramatic increase in the particle size to approximately 850 nm and 1600 nm at 4 and 24 hours respectively. This implies that the CCD formulation is not stable in salt-containing media, which was previously reported (O'Mahony et al., 2013). In contrast, CD-F-G nanoparticles maintained a particle size of less than 200 nm over the 24 hour period (**Figure 1 b**). The stability of PEGylated CD nanoparticles in salt-containing media has been previously reported, where complexes maintained their particle size in optiMEM® for up to 48 h (Evans et al., 2016b).

siRNA is subject to degradation and it is important that any vector designed for its delivery is capable of protecting its cargo from endogenous nucleases (Wittrup and Lieberman, 2015) . Thus CD-F-G and CD-M-G complexes were incubated in 10 % FBS and siRNA stability was monitored for up to 8 h. We previously reported that in the presence of FBS, free siRNA degraded in a few minutes (Evans et al., 2016b). In contrast, the presence of cyclodextrin plus PEG was capable of protecting siRNA from serum nucleases for up to 8 h (**Figure 1 c**).

The morphology of the targeted formulation (i.e. CD-F-G) was determined by TEM (**Figure 1 d**). CD-F-G gave uniform, spherical nanoparticles of approximately 200 nm in size, which reflects the results obtained by DLS (**Table 1**). DSPE-PEG_{5000} post-inserted into preformed amphiphilic CD.siRNA nanoparticles has previously been shown to result in a more spherical structure (Evans et al., 2016b).

3.2 CD-F-G Nanoparticles displayed folate-mediated uptake, a low cytotoxic profile and specific knockdown of the luciferase reporter gene *in vitro.*

Due to the heterogeneous nature of cancer, patients will respond differently to the same treatments and advances in genomics has allowed for the personalised treatment of patients based on the biology of their tumours (Van't Veer and Bernards, 2008). Two approaches are commonly utilised to target solid tumours: active targeting and passive accumulation, with both strategies showing promise at the preclinical and clinical trial stage (Sagnella et al., 2014). While passive accumulation is dependent on exploiting the properties of the tumour microenvironment (such as “leaky vasculature”), active targeting utilises a targeting ligand to exploit the overexpression of certain receptors on the surface of tumour cells (Cho et al., 2008; Lammers et al., 2008; Lammers et al., 2012).

A common targeting ligand that has been exploited for the development of cancer therapy is folate (Zwicke et al., 2012). In this study, the uptake of CD-F-G and CD-M-G nanoparticles

was assessed in prostate cancer cell lines PC3 and LNCaP cells. For both cell lines, a significant increase ($p<0.05$) in the uptake of the targeted CD-F-G compared with untargeted CD-M-G NPs (**Figure 2a and 2b**) was observed. In addition, a competition assay using excess free folate (2.5 mM) resulted in significant reductions ($p<0.01$) in the uptake of CD-F-G (44 % for PC3 and 65 % for LNCaP at 4 h). No difference in uptake was observed for CD-M-G. These results taken together would indicate that the uptake of the targeted nanoparticles is mediated (to at least some degree), by the folate ligand. Previous studies have shown that folate-targeted nanoparticles show increased uptake in both LNCaP and PC3 cells (de Oliveira et al., 2016; Evans et al., 2016b; Hattori and Maitani, 2005; Singh et al., 2009; Zhao et al., 2010). These studies highlight the benefit of targeting nanoparticles with folate for the treatment of prostate cancer.

However, the uptake of folate-targeted nanoparticles in prostate cancer can be via multiple mechanisms. The uptake of folate nanoparticles in LNCaP cells is thought to be mediated primarily by the prostate specific membrane antigen (PSMA) (Pinto et al., 1996). PSMA is a membrane bound glycoprotein, the expression of which increases as prostate cancer progresses (Evans et al., 2016a). Another advantage of targeting PSMA for prostate cancer, is that it is rapidly internalised and recycled, meaning that high concentrations of therapeutic payload can be delivered to PSMA-positive cells (Behnam Azad et al., 2015). Interestingly, it has been shown that PC3 cells lack PSMA expression and so uptake in these cells is suggested to be mediated by the reduced folate carrier (RFC), a ubiquitously expressed membrane transport system responsible for transport of folates into mammalian cells and tissues (Hattori and Maitani, 2004; Matherly and Hou, 2008). The results in **figure 2a and 2b** highlight the folate-specific uptake of CD-F-G into PC3 and LNCaP cells.

In order to be applicable for therapeutic applications, it is critical that nanoparticles are assessed for any cytotoxic effects (Lewinski et al., 2008). None of the three CD formulations used in

this study elicited significant levels of cytotoxicity in either LNCaP or PC3 cells compared with untreated controls, as analysed using the MTT assay (**Figure 2c and 2d**). The amphiphilic CD has previously been shown to be non-toxic in PC3 prostate cancer cells (Evans et al., 2015). In contrast, Lipofectamine 2000 (LIPO) resulted in significant levels of cytotoxicity in both cell lines tested over a 24 h period ($p<0.001$). While Lipofectamine 2000 has previously been shown to be a highly effective transfection agent, its use *in vivo* is limited by its toxicity (Godinho et al., 2014a).

CD-F, CD-F-G and CD-M-G formulations complexed with luciferase siRNA were used to silence a luciferase reporter gene in $PC3^{Luc}$ cells (**Figure 3**). While there was a significant level of knockdown for the CD-F formulation (55.91 ± 6.96 %), the addition of GALA to the formulation (i.e. CF-F-G) significantly increased ($P<0.05$) the level of knockdown to 76.99 ± 10.89 %. Delivery of luciferase siRNA using CD-F-G resulted in a similar level of knockdown to the positive control, Lipofectamine2000. Furthermore, there was a significantly greater level of luciferase knockdown by CD-F-G complexes compared to the CD-M-G formulation ($p<0.001$) demonstrating the effectiveness of folate-targeted nanoparticle delivery. Together, these results demonstrate the effectiveness of including PEG-Folate and GALA in the formulation and CD-F-G was chosen for further functional studies.

3.3 CD-F-G Nanoparticles resulted in specific knockdown of NRP-1 and ZEB1 and a more compact spherical structure in PC3 3D tumour spheroids.

For the therapeutic application of RNAi, the choice of target gene is critical. For the present study, two genes of interest were targeted; ZEB1 and NRP1. **Figure 4** displays the RT-PCR and western blot analysis of PC3 cells treated with CD-F-G and CD-M-G complexed with negative control, ZEB1 or NRP1 siRNA. CD-F-G resulted in a significant reduction in the levels of NRP1 mRNA (**Figure 4a**) ($P<0.05$) and ZEB1 mRNA (**Figure 4c**) ($P<0.001$) with

reductions of 50 % and 60 % respectively. While CD-M-G did show significant knockdown of ZEB1 (**Figure 4c**) ($p<0.001$), CD-F-G displayed a significantly superior level of knockdown ($P<0.05$). For functional studies, it is imperative that the genes are silenced at both the mRNA and protein levels. Using densitometry analysis, there was an approximate 60 % and 50 % reduction in NRP1 (**Figure 4b**) and ZEB1 (**Figure 4d**) protein levels, respectively, in PC3 cells treated with CD-F-G. In contrast, when treated with CD-M-G, NRP1 (**Figure 4b**) and ZEB1 (**Figure 4d**) protein levels fell by 30 % and less than 5 % respectively.

Several studies have shown that folate-targeted siRNA loaded formulations perform better in prostate cancer cell lines and tumours compared to untargeted controls. In a recent study, a PSA-responsive, folate-targeted liposomal formulation administered intravenously resulted in a significant knockdown of PLK1 mRNA and protein, resulting in significant tumour regression in a 22Rv1 xenograft tumour model (Xiang et al., 2013). Folate-targeted gold nanoparticles have been shown to result in a significant reduction in RelA mRNA in LNCaP cells, with untargeted controls displaying negligible levels of mRNA knockdown (Guo et al., 2016). A folate-targeted cyclodextrin formulation was recently shown to significantly reduce the levels of RelA mRNA in two PSMA expressing prostate cancer cell lines; LNCaP and VCaP (Evans et al., 2016b).

The combined results of the RT-PCR and western blot (**Figure 4**) highlight the superior silencing ability of the folate targeted CD (CD-F-G) over the untargeted control (i.e. CD-M-G) in silencing therapeutically relevant genes in prostate cancer cell lines.

To ascertain whether therapeutic efficacy was achieved, functional studies were performed using a 3D Matrigel™ culture to assess whether the targeted formulations complexed with NRP1 and ZEB1 siRNA reduced the infiltration of prostate cancer cells into a Matrigel™ layer (**Figure 5**). **Figure 5a** shows a representative phase contrast image of PC3 spheroids 3-4 days

following their culture onto Matrigel™, prior to any treatment with either CD-F-G or CD-M-G. Cultures treated with CD-F-G complexes resulted in more compact non-invasive colonies compared with the respective negative controls (**Figure 5b**). Interestingly, the CD-M-G complexes with NRP1 and ZEB1 siRNA did not result in a change in the invasive phenotype of the PC3 cells (**Figure 5b**), perhaps due to the inferior level of knockdown of the target protein compared with CD-F-G.

These results are consistent with previously published data. ZEB1 is a well-studied marker of epithelial to mesenchymal transition (EMT). The silencing of ZEB1 in a subpopulation of PC3 cells selected for their efficient transendothelial migration resulted in an upregulation of E-cadherin and a reduction in transendothelial migration (Drake et al., 2009). A lot of research studies have demonstrated that the EMT process is integral for the metastasis of many different carcinoma types (Heerboth et al., 2015; Hugo et al., 2007), which has highlighted the potential therapeutic benefit for silencing ZEB1 in these cancers. For example, the knockdown of ZEB1 by siRNA significantly reduces the invasion of H460 lung cancer cells *in vitro* and significantly reduces the number of lung metastases *in vivo* (Fang et al., 2014). A recent study showed that the transfection of HCC827 lung adenocarcinoma cells resulted in significantly less cells migrating through a transwell chamber (Zhang et al., 2013). Similarly the transfection of gastric adenocarcinoma AGS cells with ZEB1 siRNA significantly reduced the number of invasive colonies (Jia et al., 2012). In addition, ZEB1 siRNA was also capable of reducing the invasive activity of NOZ gallbladder cancer cells (Adachi et al., 2009).

NRP1 is another viable therapeutic target for metastatic cancer therapy. Anti-NRP1 therapy resulted in reduced VEGF-induced migration and *in vivo* neovascularization in HUVEC cells (Pan et al., 2007). For medulloblastoma, the blockade of the placental growth factor (PIGF)/NRP1 pathway result in antitumour effects *in vivo*, tumour regression, decreased metastasis and increased mouse survival (Snuderl et al., 2013). The inhibition of NRP1 (either

by inhibitor or NRP1 siRNA) reduced the migration of A549 and ACHN cells and also increased the sensitivity of the prostate cancer cell line DU145 to cisplatin and 5-FU (Jia et al., 2010). The stable knockdown of NRP1 in PC3 cells has also been shown to result in a less invasive cancer cell phenotype (Tse et al., 2017).

Conclusion

Metastatic prostate cancer still has very few treatment options, with current therapies offering only very modest increases in overall survival. In the present study, a folate-targeted modified CD-based siRNA delivery vector has been formulated with an amphiphilic fusogenic peptide, GALA, to aid in endosomal escape. The formulation is capable of binding and protecting siRNA from serum nucleases and the nanoparticles are capable of resisting aggregation for up to 24 h in salt-containing medium. The nanoparticles show folate-mediated uptake in two prostate cancer cell lines with reported different folate uptake mechanisms (Hattori and Maitani, 2004, 2005). Folate-targeted complexes show specific knockdown of a luciferase reporter gene and two target genes (NRP1 and ZEB1) in the metastatic prostate cancer PC3 cell line. Initial functional studies of PC3 tumour spheroids have shown that knockdown of NRP1 and ZEB1 by CD-F-G resulted in more compact colonies and reduced infiltration into the underlying Matrigel™ layer. To our knowledge, this is the first example of a folate-targeted CD vector used to silence therapeutically relevant genes in a 3D tumour spheroid model of prostate cancer.

Acknowledgements

This work is supported by the Irish Cancer Society via a Research Scholarship to JCE (CRS12EVA) and a Project Grant to COD (PCI11ODR). The authors would also like to acknowledge funding from Irish Research Council (GOIPD/2014/151) for research funding and FRSQ postdoctoral fellowship to MM. BGH, CCN and KS would like to acknowledge funding from the NHMRC (APP1100417), Cancer Australia, Cure Cancer Australia

Foundation, the Australian Government Department of Health as well as the Movember Foundation and the Prostate Cancer Foundation of Australia through a Movember Revolutionary Team Award.

Figure Legends

Figure 1. Assessment of CD complexes in media and morphology of CD.siRNA structures by TEM; *a) siRNA binding assay with i) naked siRNA, ii) CCD, iii) CD-F-G and iv) CD-M-G. Naked siRNA (i) has migrated through the gel. However for the three formulations tested, the siRNA did not migrate through the well, highlighting that it is bound by the CD complexes b) Stability of CCD and CD-F-G nanoparticles in 90 % optiMEM® over 24 h, c) Stability of CD-F-G (top) and CD-M-G (bottom) in 10 % FBS. d) TEM images of CD-F-G; magnification x100k scale 200nm*

Figure 2: Competitive uptake of cyclodextrin nanoparticles and comparing cytotoxicity of cyclodextrin nanoparticles and Lipofectamine 2000 in PC3 and LNCaP cells: *Uptake of 6-FAM-labelled siRNA (50 nM) into a) PC3 and b) LNCaP cells either with no pre-treatment or pre-treated with 2.5 mM free folic acid 1 h prior to transfection. Uptake of CD-F-G nanoparticles was significantly reduced in the presence of free folic acid. Toxicity of CD nanoparticles was assessed by MTT 24 h following treatment in c) PC3 and d) LNCaP cells.*

Figure 3: Knockdown of luciferase reporter gene in PC3 cells by Lipofectamine2000 (LIPO), targeted (CD-F-G, CD-F) and untargeted complexes (CD-M-G). *Luciferase gene knockdown by Lipofectamine2000 and Cyclodextrin nanoparticles was normalised to the respective siRNA negative control counterpart. CD-F-G nanoparticles complexed with luciferase siRNA resulted in a significant level of luciferase knockdown compared to both CD-M-G and CD-F. Data are presented as mean ± SD (***$p<0.001$, $n=3$).*

Figure 4: CD-F-G complexed with ZEB1 and NRP1 siRNA results in significant levels of mRNA and protein knockdown assessed by RT-PCR and western blot in PC3 cells. *Following transfection of PC3 cells with cyclodextrin nanoparticles complexed with NRP1 or ZEB1 siRNA, the relative mRNA knockdown and protein suppression levels were confirmed by RT-PCR (a, c) and western blot analysis (b, d). For CD formulations, knockdown was compared with its equivalent non-silencing control (*p<0.05, ***p<0.001). Data are presented as mean ± SD (n=4-6).*

Figure 5: Representative phase-contrast images of PC3 cells grown in a 3D Matrigel™ culture at 96 h post treatment. *Representative images of PC3 spheroids prior to treatment a), PC3 spheroids were treated with either b) CD-F-G or c) CD-M-G complexed with non-silencing, NRP1 or ZEB1 siRNA at t= 96 h (scale bar=100 μM). The silencing of NRP1 and ZEB1 by CD-F-G complexes result in more compact, spherical colonies compared to non-silencing controls and CD-M-G controls*

Table Legends

Table 1. Size and charge of CD.siRNA complexes*. Physicochemical properties of CD.siRNA complexes with the incorporation of DSPE-PEG$_{5000}$ and the amphiphilic peptide GALA by the post-insertion method. Data is presented as the mean ± SD (n=3).*

References

A do Carmo, F., C Sathler, P., Zancan, P., R Rodrigues, C., C Castro, H., P de Sousa, V., Sola-Penna, M., M Cabral, L., 2014. Therapeutic nanosystems for oral administration of insulin. Current pharmaceutical biotechnology 15, 620-628.

Adachi, Y., Takeuchi, T., Nagayama, T., Ohtsuki, Y., Furihata, M., 2009. Zeb1-mediated T-cadherin repression increases the invasive potential of gallbladder cancer. FEBS letters 583, 430-436.

Aranda, C., Urbiola, K., Ardoy, A.M., Fernández, J.M.G., Mellet, C.O., de Ilarduya, C.T., 2013. Targeted gene delivery by new folate–polycationic amphiphilic cyclodextrin–DNA nanocomplexes in vitro and in vivo. European Journal of Pharmaceutics and Biopharmaceutics 85, 390-397.

Behnam Azad, B., Banerjee, S.R., Pullambhatla, M., Lacerda, S., Foss, C.A., Wang, Y., Ivkov, R., Pomper, M.G., 2015. Evaluation of a PSMA-targeted BNF nanoparticle construct. Nanoscale 7, 4432-4442.

Cho, K., Wang, X., Nie, S., Shin, D.M., 2008. Therapeutic nanoparticles for drug delivery in cancer. Clinical cancer research 14, 1310-1316.

Davis, M.E., 2009. The first targeted delivery of siRNA in humans via a self-assembling, cyclodextrin polymer-based nanoparticle: from concept to clinic. Molecular pharmaceutics 6, 659-668.

de Oliveira, L.F., Bouchmella, K., Gonçalves, K.d.A., Bettini, J., Kobarg, J.r., Cardoso, M.B., 2016. Functionalized silica nanoparticles as an alternative platform for targeted drug-delivery of water insoluble drugs. Langmuir 32, 3217-3225.

Drake, J.M., Strohbehn, G., Bair, T.B., Moreland, J.G., Henry, M.D., 2009. ZEB1 enhances transendothelial migration and represses the epithelial phenotype of prostate cancer cells. Molecular biology of the cell 20, 2207-2217.

Evans, J.C., Malhotra, M., Cryan, J.F., O'Driscoll, C.M., 2016a. The therapeutic and diagnostic potential of the prostate specific membrane antigen/glutamate carboxypeptidase II (PSMA/GCPII) in cancer and neurological disease. Br J Pharmacol.

Evans, J.C., Malhotra, M., Guo, J., O'Shea, J.P., Hanrahan, K., O'Neill, A., Landry, W.D., Griffin, B.T., Darcy, R., Watson, R.W., O'Driscoll, C.M., 2016b. Folate-targeted amphiphilic cyclodextrin.siRNA nanoparticles for prostate cancer therapy exhibit PSMA mediated uptake, therapeutic gene silencing in vitro and prolonged circulation in vivo. Nanomedicine: Nanotechnology, Biology and Medicine 12, 2341-2351.

Evans, J.C., McCarthy, J., Torres-Fuentes, C., Cryan, J.F., Ogier, J., Darcy, R., Watson, R.W., O'Driscoll, C.M., 2015. Cyclodextrin mediated delivery of NF-kappaB and SRF siRNA reduces the invasion potential of prostate cancer cells in vitro. Gene Ther 22, 802-810.

Fang, S., Wu, L., Li, M., Yi, H., Gao, G., Sheng, Z., Gong, P., Ma, Y., Cai, L., 2014. ZEB1 knockdown mediated using polypeptide cationic micelles inhibits metastasis and effects sensitization to a chemotherapeutic drug for cancer therapy. Nanoscale 6, 10084-10094.

Fischer, K.R., Durrans, A., Lee, S., Sheng, J., Li, F., Wong, S.T., Choi, H., El Rayes, T., Ryu, S., Troeger, J., 2015. Epithelial-to-mesenchymal transition is not required for lung metastasis but contributes to chemoresistance. Nature 527, 472-476.

Fitzgerald, K.A., Malhotra, M., Gooding, M., Sallas, F., Evans, J.C., Darcy, R., O'Driscoll, C.M., 2016. A novel, anisamide-targeted cyclodextrin nanoformulation for siRNA delivery to prostate cancer cells expressing the sigma-1 receptor. International journal of pharmaceutics 499, 131-145.

Godinho, B.M., Ogier, J.R., Darcy, R., O'Driscoll, C.M., Cryan, J.F., 2013. Self-assembling modified beta-cyclodextrin nanoparticles as neuronal siRNA delivery vectors: focus on Huntington's disease. Mol Pharm 10, 640-649.

Godinho, B.M.D.C., McCarthy, D.J., Torres-Fuentes, C., Beltrán, C.J., McCarthy, J., Quinlan, A., Ogier, J.R., Darcy, R., O'Driscoll, C.M., Cryan, J.F., 2014a. Differential nanotoxicological and neuroinflammatory liabilities of non-viral vectors for RNA interference in the central nervous system. Biomaterials 35, 489-499.

Godinho, B.M.D.C., Ogier, J.R., Quinlan, A., Darcy, R., Griffin, B.T., Cryan, J.F., O'Driscoll, C.M., 2014b. PEGylated cyclodextrins as novel siRNA nanosystems: Correlations between polyethylene glycol length and nanoparticle stability. International Journal of Pharmaceutics 473, 105-112.

Graziani, G., Lacal, P.M., 2015. Neuropilin-1 as therapeutic target for malignant melanoma. Frontiers in Oncology 5.

Gref, R., Lück, M., Quellec, P., Marchand, M., Dellacherie, E., Harnisch, S., Blunk, T., Müller, R., 2000. 'Stealth'corona-core nanoparticles surface modified by polyethylene glycol (PEG): influences of the corona (PEG chain length and surface density) and of the core composition on phagocytic uptake and plasma protein adsorption. Colloids and Surfaces B: Biointerfaces 18, 301-313.

Guo, J., O'Driscoll, C.M., Holmes, J.D., Rahme, K., 2016. Bioconjugated gold nanoparticles enhance cellular uptake: A proof of concept study for siRNA delivery in prostate cancer cells. International journal of pharmaceutics 509, 16-27.
Guo, J., Ogier, J.R., Desgranges, S., Darcy, R., O'Driscoll, C., 2012. Anisamide-targeted cyclodextrin nanoparticles for siRNA delivery to prostate tumours in mice. Biomaterials 33, 7775-7784.
Hattori, Y., Maitani, Y., 2004. Enhanced in vitro DNA transfection efficiency by novel folate-linked nanoparticles in human prostate cancer and oral cancer. J Control Release 97, 173-183.
Hattori, Y., Maitani, Y., 2005. Folate-linked nanoparticle-mediated suicide gene therapy in human prostate cancer and nasopharyngeal cancer with herpes simplex virus thymidine kinase. Cancer Gene Ther 12, 796-809.
Hay, E., 1995. An overview of epithelio-mesenchymal transformation. Cells Tissues Organs 154, 8-20.
Heerboth, S., Housman, G., Leary, M., Longacre, M., Byler, S., Lapinska, K., Willbanks, A., Sarkar, S., 2015. EMT and tumor metastasis. Clinical and translational medicine 4, 1.
Hugo, H., Ackland, M.L., Blick, T., Lawrence, M.G., Clements, J.A., Williams, E.D., Thompson, E.W., 2007. Epithelial—mesenchymal and mesenchymal—epithelial transitions in carcinoma progression. Journal of cellular physiology 213, 374-383.
Jambhekar, S.S., Breen, P., 2016a. Cyclodextrins in pharmaceutical formulations I: structure and physicochemical properties, formation of complexes, and types of complex. Drug discovery today 21, 356-362.
Jambhekar, S.S., Breen, P., 2016b. Cyclodextrins in pharmaceutical formulations II: solubilization, binding constant, and complexation efficiency. Drug discovery today 21, 363-368.
Jia, B., Liu, H., Kong, Q., Li, B., 2012. Overexpression of ZEB1 associated with metastasis and invasion in patients with gastric carcinoma. Molecular and cellular biochemistry 366, 223-229.
Jia, H., Cheng, L., Tickner, M., Bagherzadeh, A., Selwood, D., Zachary, I., 2010. Neuropilin-1 antagonism in human carcinoma cells inhibits migration and enhances chemosensitivity. British journal of cancer 102, 541-552.
Lammers, T., Hennink, W., Storm, G., 2008. Tumour-targeted nanomedicines: principles and practice. British journal of cancer 99, 392-397.
Lammers, T., Kiessling, F., Hennink, W.E., Storm, G., 2012. Drug targeting to tumors: principles, pitfalls and (pre-) clinical progress. Journal of controlled release 161, 175-187.
Latil, A., Bieche, I., Pesche, S., Valeri, A., Fournier, G., Cussenot, O., Lidereau, R., 2000. VEGF overexpression in clinically localized prostate tumors and neuropilin-1 overexpression in metastatic forms. International journal of cancer 89, 167-171.
Lewinski, N., Colvin, V., Drezek, R., 2008. Cytotoxicity of nanoparticles. small 4, 26-49.
Li, W., Nicol, F., Szoka, F.C., 2004. GALA: a designed synthetic pH-responsive amphipathic peptide with applications in drug and gene delivery. Advanced drug delivery reviews 56, 967-985.
Matherly, L.H., Hou, Z., 2008. Structure and function of the reduced folate carrier: a paradigm of a major facilitator superfamily mammalian nutrient transporter. Vitamins & Hormones 79, 145-184.
McCarthy, J., O'Neill, M.J., Bourre, L., Walsh, D., Quinlan, A., Hurley, G., Ogier, J., Shanahan, F., Melgar, S., Darcy, R., O'Driscoll, C.M., 2013. Gene silencing of TNF-alpha in a murine model of acute colitis using a modified cyclodextrin delivery system. Journal of Controlled Release 168, 28-34.
Meredith, M.E., Salameh, T.S., Banks, W.A., 2015. Intranasal delivery of proteins and peptides in the treatment of neurodegenerative diseases. The AAPS journal 17, 780-787.
Monfardini, C., Veronese, F.M., 1998. Stabilization of substances in circulation. Bioconjugate chemistry 9, 418-450.
O'Mahony, A.M., Desgranges, S., Ogier, J., Quinlan, A., Devocelle, M., Darcy, R., Cryan, J.F., O'Driscoll, C.M., 2013. In vitro investigations of the efficacy of cyclodextrin-siRNA complexes modified with lipid-PEG-Octaarginine: towards a formulation strategy for non-viral neuronal siRNA delivery. Pharm Res 30, 1086-1098.

O'Mahony, A.M., Doyle, D., Darcy, R., Cryan, J.F., O'Driscoll, C.M., 2012a. Characterisation of cationic amphiphilic cyclodextrins for neuronal delivery of siRNA: effect of reversing primary and secondary face modifications. European Journal of Pharmaceutical Sciences 47, 896-903.

O'Mahony, A.M., Godinho, B.M.D.C., Ogier, J., Devocelle, M., Darcy, R., Cryan, J.F., O'Driscoll, C.M., 2012b. Click-Modified Cyclodextrins as Nonviral Vectors for Neuronal siRNA Delivery. ACS Chemical Neuroscience 3, 744-752.

Pan, Q., Chanthery, Y., Liang, W.-C., Stawicki, S., Mak, J., Rathore, N., Tong, R.K., Kowalski, J., Yee, S.F., Pacheco, G., 2007. Blocking neuropilin-1 function has an additive effect with anti-VEGF to inhibit tumor growth. Cancer cell 11, 53-67.

Parente, R.A., Nadasdi, L., Subbarao, N.K., Szoka Jr, F.C., 1990. Association of a pH-sensitive peptide with membrane vesicles: role of amino acid sequence. Biochemistry 29, 8713-8719.

Pellet-Many, C., Frankel, P., Jia, H., Zachary, I., 2008. Neuropilins: structure, function and role in disease. Biochemical Journal 411, 211-226.

Pinto, J.T., Suffoletto, B.P., Berzin, T.M., Qiao, C.H., Lin, S., Tong, W.P., May, F., Mukherjee, B., Heston, W., 1996. Prostate-specific membrane antigen: a novel folate hydrolase in human prostatic carcinoma cells. Clinical Cancer Research 2, 1445-1451.

Sagnella, S.M., McCarroll, J.A., Kavallaris, M., 2014. Drug delivery: beyond active tumour targeting. Nanomedicine: Nanotechnology, Biology and Medicine 10, 1131-1137.

Siegel, R.L., Miller, K.D., Jemal, A., 2015. Cancer statistics, 2015. CA: a cancer journal for clinicians 65, 5-29.

Simoes, S., Slepushkin, V., Gaspar, R., Pedroso de Lima, M., Düzgüneş, N., 1998. Gene delivery by negatively charged ternary complexes of DNA, cationic liposomes and transferrin or fusigenic peptides. Gene therapy 5.

Simoes, S., Slepushkin, V., Pires, P., Gaspar, R., de Lima, M.P., Düzgüneş, N., 1999a. Mechanisms of gene transfer mediated by lipoplexes associated with targeting ligands or pH-sensitive peptides. Gene therapy 6, 1798-1807.

Simoes, S., Slepushkin, V., Pretzer, E., Dazin, P., Gaspar, R., de Lima, M.P., Düzgüneş, N., 1999b. Transfection of human macrophages by lipoplexes via the combined use of transferrin and pH-sensitive peptides. Journal of leukocyte biology 65, 270-279.

Singh, R., Singh, S., Sharma, P.K., Lillard Jr, J.W., 2009. T regulatory and prostate cancer cell-specific drug targeting using novel XPclad© nanoparticles (42.7). The Journal of Immunology 182, 42.47-42.47.

Snuderl, M., Batista, A., Kirkpatrick, N.D., de Almodovar, C.R., Riedemann, L., Walsh, E.C., Anolik, R., Huang, Y., Martin, J.D., Kamoun, W., 2013. Targeting placental growth factor/neuropilin 1 pathway inhibits growth and spread of medulloblastoma. Cell 152, 1065-1076.

Song, E., Lee, S.-K., Wang, J., Ince, N., Ouyang, N., Min, J., Chen, J., Shankar, P., Lieberman, J., 2003. RNA interference targeting Fas protects mice from fulminant hepatitis. Nature medicine 9, 347-351.

Subbarao, N.K., Parente, R.A., Szoka Jr, F.C., Nadasdi, L., Pongracz, K., 1987. The pH-dependent bilayer destabilization by an amphipathic peptide. Biochemistry 26, 2964-2972.

Tse, B., Volpert, M., Ratther, E., Stylianou, N., Nouri, M., McGowan, K., Lehman, M., McPherson, S., Roshan-Moniri, M., Butler, M., 2017. Neuropilin-1 is upregulated in the adaptive response of prostate tumors to androgen-targeted therapies and is prognostic of metastatic progression and patient mortality. Oncogene 36, 3417.

Van't Veer, L.J., Bernards, R., 2008. Enabling personalized cancer medicine through analysis of gene-expression patterns. Nature 452, 564-570.

Wittrup, A., Lieberman, J., 2015. Knocking down disease: a progress report on siRNA therapeutics. Nat Rev Genet 16, 543-552.

Xiang, B., Dong, D.-W., Shi, N.-Q., Gao, W., Yang, Z.-Z., Cui, Y., Cao, D.-Y., Qi, X.-R., 2013. PSA-responsive and PSMA-mediated multifunctional liposomes for targeted therapy of prostate cancer. Biomaterials 34, 6976-6991.

Yacoub, M., Coulon, A., Celhay, O., Irani, J., Cussenot, O., Fromont, G., 2009. Differential expression of the semaphorin 3A pathway in prostatic cancer. Histopathology 55, 392-398.

Yao, D., Dai, C., Peng, S., 2011. Mechanism of the mesenchymal–epithelial transition and its relationship with metastatic tumor formation. Molecular Cancer Research 9, 1608-1620.
Zhang, J., Lu, C., Zhang, J., Kang, J., Cao, C., Li, M., 2013. Involvement of ZEB1 and E-cadherin in the invasion of lung squamous cell carcinoma. Molecular biology reports 40, 949-956.
Zhang, P., Sun, Y., Ma, L., 2015. ZEB1: at the crossroads of epithelial-mesenchymal transition, metastasis and therapy resistance. Cell Cycle 14, 481-487.
Zhao, D., Zhao, X., Zu, Y., Li, J., Zhang, Y., Jiang, R., Zhang, Z., 2010. Preparation, characterization, and in vitro targeted delivery of folate-decorated paclitaxel-loaded bovine serum albumin nanoparticles. Int J Nanomedicine 5, 669-677.
Zheng, X., Carstens, J.L., Kim, J., Scheible, M., Kaye, J., Sugimoto, H., Wu, C.-C., LeBleu, V.S., Kalluri, R., 2015. Epithelial-to-mesenchymal transition is dispensable for metastasis but induces chemoresistance in pancreatic cancer. Nature 527, 525-530.
Zwicke, G.L., Mansoori, G.A., Jeffery, C.J., 2012. Utilizing the folate receptor for active targeting of cancer nanotherapeutics. Nano Reviews & Experiments 3.

Figure Caption

Figr-1

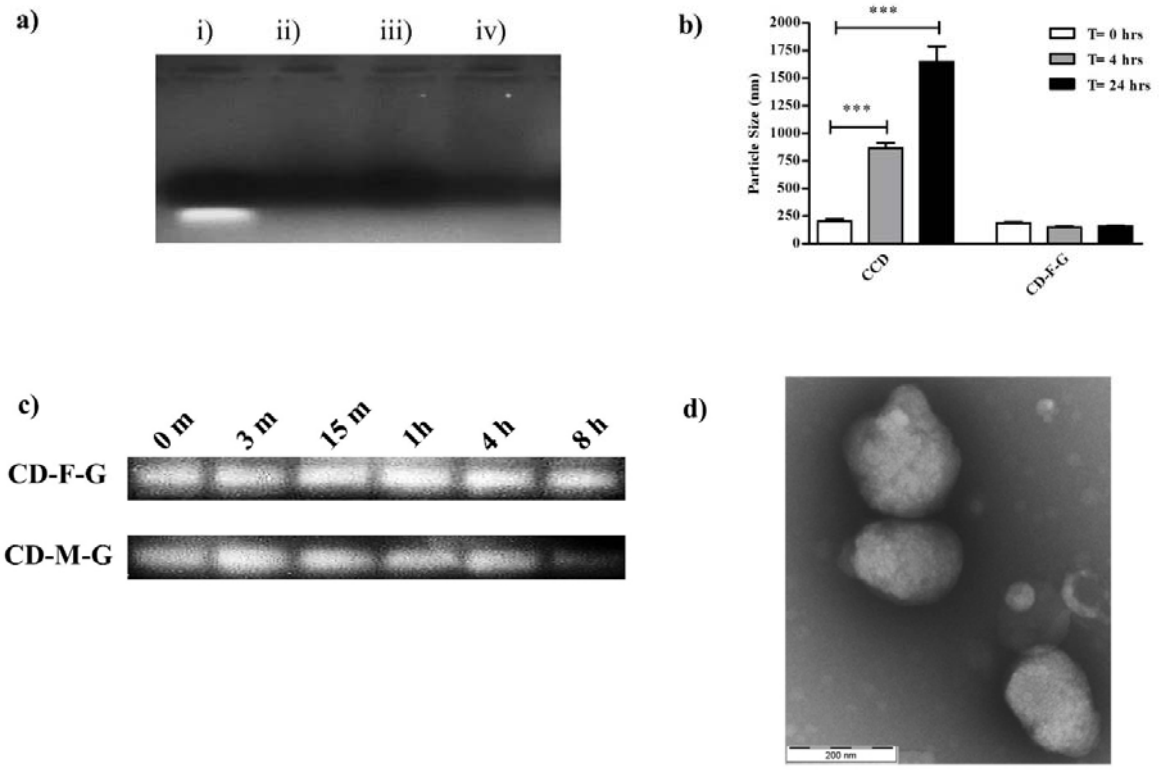

Figr-2

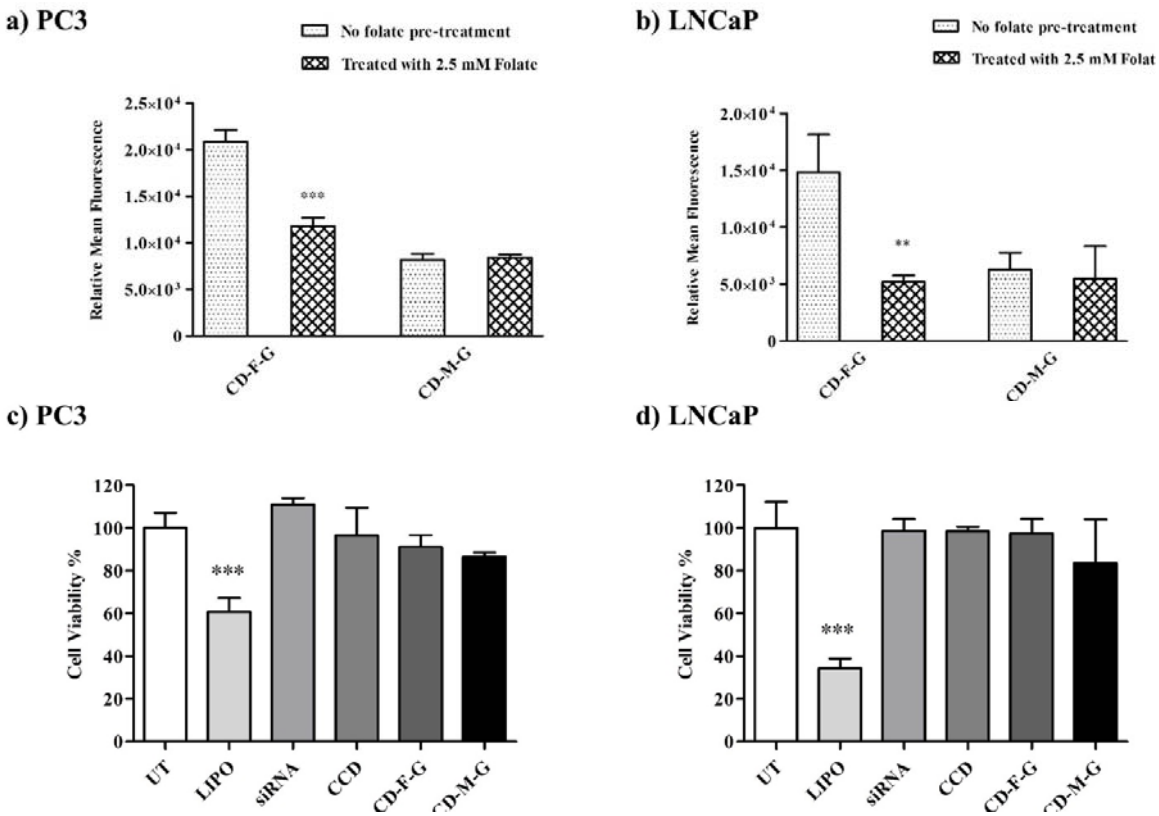

Figr-3

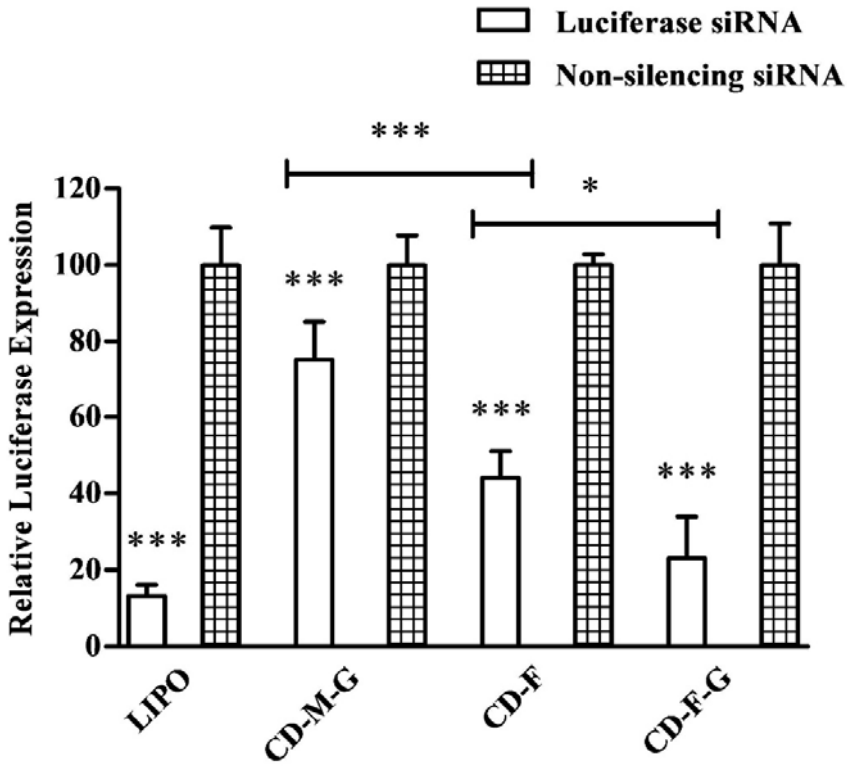

Figr-4

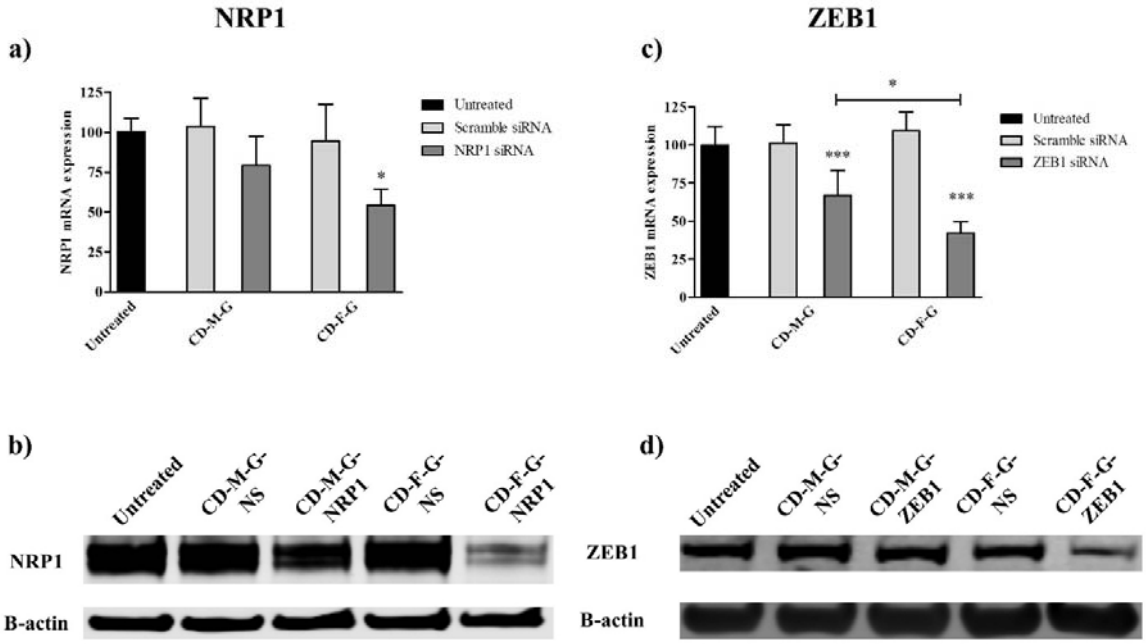

Figr-5

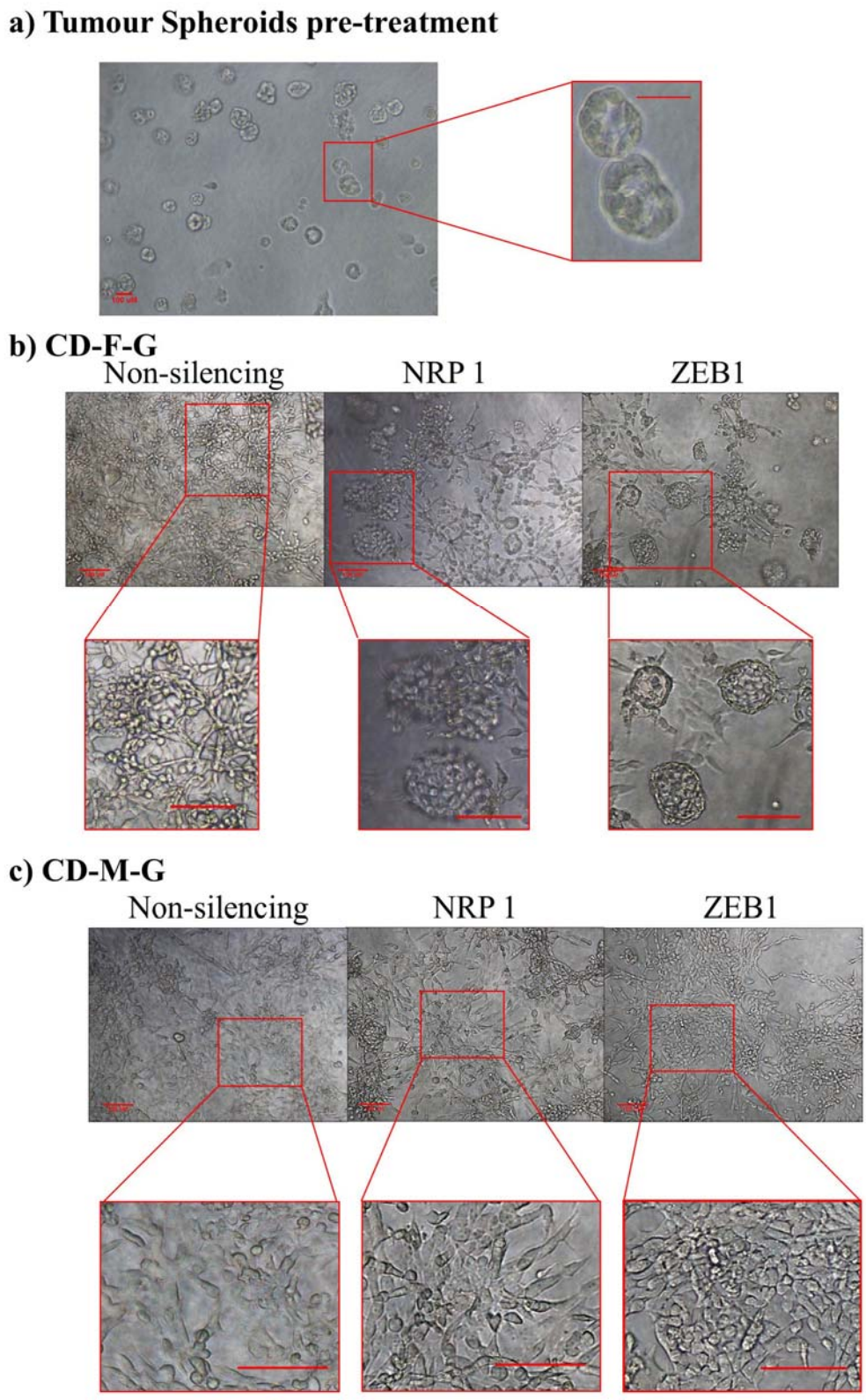

Formulation	CD:DPF:DPM:GALA molar ratio	Particle size (nm)	PDI	Zeta potential
CCD	1:0:0:0	202.76 ± 20.41	0.33 ± 0.04	46.42 ± 1.67
CD-M-G	1:0:0.75:0.05	128.66 ± 10.31	0.23 ± 0.02	-9.07 ± 1.31
CD-F	1:0.75:0:0	154.5 ± 35.79	0.26 ± 0.07	30.32 ± 2.44
CD-F-G	1:0.75:0:0.05	187.99 ± 10.02	0.13 ± 0.06	0.67 ± 2.66